Received: 30 September 2021 | Revised: 4 November 2021 | Accepted: 4 November 2021

DOI: 10.1111/joa.13593

Journal of Anatomy ANATOMICAL SOCIETY WILEY

ORIGINAL PAPER

Neurosensory anatomy of Varanopidae and its implications for early synapsid evolution

Kayla D. Bazzana[1,2] | David C. Evans[2,3] | Joseph J. Bevitt[4] | Robert R. Reisz[1,5]

[1]Department of Biology, University of Toronto Mississauga, Mississauga, Canada

[2]Department of Natural History, Royal Ontario Museum, Toronto, Canada

[3]Department of Ecology and Evolutionary Biology, University of Toronto, Toronto, Canada

[4]Australian Centre for Neutron Scattering, Australian Nuclear Science and Technology Organisation, Lucas Heights, New South Whales, Australia

[5]International Center of Future Science, Dinosaur Evolution Research Center, Jilin University, Changchun, Jilin Province, China

Correspondence
Kayla D. Bazzana, Department of Biology, William G. Davis Building, University of Toronto Mississauga, 3359 Mississauga Rd., Mississauga L5L 1C6, ON, Canada.
Email: kayla.bazzana@mail.utoronto.ca

Funding information
Natural Sciences and Engineering Research Council of Canada

Abstract

Varanopids are a group of Palaeozoic terrestrial amniotes which represent one of the earliest-diverging groups of synapsids, but their palaeoneurology has gone largely unstudied and recent analyses have challenged their traditional placement within synapsids. We utilized computed tomography (CT) to study the virtual cranial and otic endocasts of six varanopids, including representative taxa of both mycterosaurines and varanodontines. Our results show that the varanopid brain is largely plesiomorphic, being tubular in shape and showing no expansion of the cerebrum or olfactory bulbs, but is distinct in showing highly expanded floccular fossae. The housing of the varanopid bony labyrinth is also distinct, in that the labyrinth is bounded almost entirely by the supraoccipital-opisthotic complex, with the prootic only bordering the ventral portion of the vestibule. The bony labyrinth is surprisingly well-ossified, clearly preserving the elliptical, sub-orthogonal canals, prominent ampullae, and the short, undifferentiated vestibule; this high degree of ossification is similar to that seen in therapsid synapsids and supports the traditional placement of varanopids within Synapsida. The enlarged anterior canal, together with the elliptical, orthogonal canals and enlarged floccular fossa, lend support for the fast head movements indicated by the inferred predatory feeding mode of varanopids. Reconstructed neurosensory anatomy indicates that varanopids may have a much lower-frequency hearing range compared to more derived synapsids, suggesting that, despite gaining some active predatory features, varanopids retain plesiomorphic hearing capabilities. As a whole, our data reveal that the neuroanatomy of pelycosaur-grade synapsids is far more complex than previously anticipated.

KEYWORDS
bony labyrinth, computed tomography, palaeoneurology, Permian, Synapsida

1 | INTRODUCTION

Extant terrestrial vertebrate communities are dominated by amniotes, both sauropsids (non-avian reptiles and birds) and synapsids (mammals). Although mammals are the only remaining synapsids, there is a rich fossil record of synapsid taxa extending back to the late Carboniferous, including many groups with no extant descendants. Studying these fossil taxa is essential for identifying the key palaeobiological attributes that led to the eventual rise of crown mammals. The palaeoneurology of non-mammalian synapsids and the evolution of the ear, in particular, are especially important for understanding synapsid palaeobiology (Benoit, Adnet, et al., 2013 Benoit, Mabrouk, et al., 2013 Benoit, Merigeaud, et al., 2013; Ekdale, 2013; Kemp, 2016; Luo et al., 2016; Stokstad, 2003; Walsh et al., 2009) and are of particular interest for characterizing both the plesiomorphic condition and the stepwise acquisition of crown mammalian features.

The study of synapsid neuroevolution has historically been heavily skewed towards characterizing the progressive evolution of the mammalian middle ear from the postdentary bones of therapsids (Allin, 1975; Kemp, 2005, 2016; Luo, 2011; Luo et al., 2016; Ramírez-Chaves et al., 2016; Rubidge & Sidor, 2001). Relatively less attention has been given to the inner ear, which is unsurprising given that study of the inner ear is substantially more difficult to achieve through non-destructive external examination and is based on the reconstruction of soft tissues from osteological correlates. In contrast, the hard tissue components of the middle ear are generally externally visible and represent the actual structures of interest. However, since the advent of the widespread usage of computed tomography (CT) in palaeontological analyses (Conroy & Vanier, 1984; Klembara et al., 2020; Marino et al., 2003; Rogers, 1999; Szostakiwskyj et al., 2015; Witmer et al., 2008), researchers have been able to analyse internal anatomical features and to reconstruct virtual endocasts of the brain cavity and inner ear, allowing us to approximate the morphology of the now-lost soft tissues themselves.

The ability to reconstruct cranial and otic endocasts is particularly important for the study of synapsid evolution. Because the inner ear houses organs for both audition and balance, its morphology can inform on several aspects of an animal's palaeobiology, including auditory abilities (Laaß, 2015a,b, 2016; Manoussaki et al., 2008; Walsh et al., 2009), locomotor style (Silcox et al., 2009; Spoor et al., 2002, 2007), head posture (Sereno et al., 2007; Benoit, Manger, Norton et al., 2017; but see Benoit et al., 2020 for criticism of this practice), adaptations to secondarily aquatic lifestyles (Benoit, Adnet, et al., 2013; Georgi et al., 2013; Neenan & Scheyer, 2012; Spoor et al., 2002), and can provide insights regarding social behaviours and communication (Benoit, Merigeaud, et al., 2013; Evans et al., 2009; Walsh et al., 2009). The inner ear has also been used to inform phylogenetic reconstructions (Benoit, Merigeaud, et al., 2013; Lebrun et al., 2010). Looking specifically at mammals, the inner ear is unique in displaying a highly elongated, frequently coiled cochlea equivalent to the short reptilian lagena (Allin & Hopson, 1992). Given its uniqueness, the evolution of the mammalian ear has been the subject of extensive study, and the palaeoneurology of non-mammalian therapsids has received similar considerable attention (Benoit, Fernandez, et al., 2017; Benoit, Manger, Fernandez, et al., 2017; Benoit, Manger, Norton et al., 2017; Laaß, 2015a,b). However, comparatively little attention has been given to their precursors, the pelycosaur-grade synapsids.

Pelycosaurian synapsids are known primarily from the Late Carboniferous and early Permian of Europe and North America (Maho et al., 2019; Reisz, 1986), with a small number of taxa present in the middle Permian of Russia and South Africa (Modesto et al., 2001; Reisz et al., 1998). Therapsida, the clade of derived synapsids which includes mammals, first appears in the late Permian of Russia (Ivahknenko et al., 1997) and South Africa (Rubidge, 1990, 1995) and is believed to have diverged from the pelycosaur-grade sphenacodontids (Rubidge & Sidor, 2001). Despite the importance of pelycosaur-grade synapsids as the predecessors to therapsids, their palaeoneurology has been largely neglected in studies of synapsid evolution. This is somewhat unsurprising, as most non-mammalian synapsids do not display the same degree of braincase ossification seen in mammals (Benoit, Fernandez, et al., 2017); as a result, large portions of the anterior braincase are often not preserved, rendering the production of a complete endocast largely impossible. However, the posterior braincase, including the otic capsules, is more likely to preserve and thus we can still glean valuable information regarding the palaeobiology of these earliest synapsids.

Varanopidae represents one of the earliest-diverging, and one of the most widely dispersed, synapsid clades, both temporally, spanning the late Pennsylvanian to the middle late Permian, and geographically, with localities in North America, Europe, Russia, and South Africa (Campione & Reisz, 2010; Reisz & Dilkes, 2003; Reisz & Modesto, 2007). Although they have traditionally been considered to be basal synapsids (Romer & Price, 1940; Spindler et al., 2018), recent analyses have challenged this view, suggesting that they may be part of Diapsida (Ford & Benson, 2020). Given the current and increasing emphasis on the utility of neurocranial anatomy for informing phylogenetic interpretations (Klembara et al., 2020; Pardo et al., 2017), clarifying the hard- and soft-tissue anatomy of the neurocranium of these early amniotes may provide additional insights into discussions of the placement of varanopids within crown Amniota. Furthermore, as one of the earliest-diverging groups of synapsids, varanopids reflect an important phase of synapsid evolution, and clarifying the palaeoneurology of these early synapsids is important for establishing the plesiomorphic palaeoneurological condition for Therapsida. Refining our understanding of varanopid ecology and palaeobiology is critical for accurate contextualization of later synapsid evolution, and palaeoneurology represents an important, yet largely unexplored, source of this kind of information. Here we describe the virtual cranial and otic endocasts of the main groups of varanopids, Mycterosaurinae and Varanodontinae, providing the first virtual endocast-based description of the brain and inner ear of any pelycosaurian synapsids, and discuss the broader implications of the results.

2 | METHODS

2.1 | Specimens

The skulls and isolated braincases of six varanopids were scanned via neutron computed tomography (*Mycterosaurus*, ROMVP86543, ROMVP87043, and *Aerosaurus*) and by X-ray computed tomography (*Mycterosaurus* and *Varanodon*).

The mycterosaurine varanopids are represented by four specimens:

- OMNH 73209 *Mesenosaurus efremovi* Maho, Gee, and Reisz, 2019; nearly complete skull and mandible with braincase preserving the supraoccipital-opisthotic complex, occiput, prootics, parasphenoid, and the right paroccipital process.

- FMNH UC 692 *Mycterosaurus longiceps* Williston, 1915; nearly complete skull with braincase preserving the supraoccipital-opisthotic complex, occiput, prootics, and parasphenoid.
- ROMVP86543 indeterminate mycterosaurine; isolated braincase preserving the supraoccipital-opisthotic complex, occiput, prootics, parasphenoid plate, and the proximal portions of both paroccipital processes.
- ROMVP87043 indeterminate mycterosaurine; isolated braincase preserving the supraoccipital-opisthotic complex, occiput, prootics, parasphenoid plate, and proximal portions of both paroccipital processes.

The varanodontine varanopids are represented by two specimens:

- UCMP 35762 *Aerosaurus wellesi* Langston & Reisz, 1981; isolated braincase preserving the supraoccipital-opisthotic complex, occiput, prootics, parasphenoid plate, paroccipital processes, and lateral processes of the supraoccipital.
- FMNH UR 986 *Varanodon agilis* Olson, 1965; nearly complete skull including the braincase.

2.2 | Scanning

Aerosaurus, *Mesenosaurus*, ROMVP86543 and ROMVP87043 were scanned at the DINGO neutron radiography/tomography/imaging station, located on the thermal HB 2 beam, tangentially facing the 20 MW Open- Pool Australian Lightwater (OPAL) reactor housed at the Australian Nuclear Science and Technology Organisation (ANSTO), Lucas Heights, New South Wales, Australia.

The DINGO facility utilises a quasi-parallel collimated beam of thermal neutrons from OPAL with a maximum spectrum intensity at 1.08 Å (70 meV) and full-width-at-half-maximum (FWHM) of 0.9 Å (100 meV). For *Mesenosaurus*, ROMVP86543, and ROMVP87043 a collimation ratio (*L*/*D*) of 1000 (Garbe et al., 2015) was used to ensure highest available spatial resolution, where *L* is the neutron aperture-to-sample length and *D* is the neutron aperture diameter. The field of view was set to 100 × 100 mm^2 with a voxel size of 45.5 × 45.5 × 45.5 μm for *Mesenosaurus*, ROMVP86543, and ROMVP87043; for *Aerosaurus*, the field of view was 95 × 80 mm^2 with a voxel size of 37 × 37 × 37 μm. Neutrons were converted to photons with a 30μm thick terbium-doped Gadox scintillator screen (Gd_2O_2S:Tb, RC Tritec AG); photons were then detected by an Andor IKON-L CCD camera (liquid cooled, 16-bit, 2048 × 2048 pixels) coupled with a Makro Planar 50 mm (for *Mesenosaurus* and *Aerosaurus*) and 100 mm (for ROMVP86543 and ROMVP87043) Carl Zeiss lens. For *Aerosaurus*, an ANDOR Neo 5.5 sCMOS camera (16-bit, 2560 × 2160 pixels) was used. For *Mesenosaurus*, a total of 1000 equally-spaced angle shadow-radiograph were obtained every 0.18° as the sample was rotated 180° about its vertical axis; for ROMVP86543 and ROMVP87043, a total of 800 radiographs were obtained every 0.225°. For *Aerosaurus*, 900 radiographs were obtained every 0.2°. Both dark (closed shutter) and beam profile (open shutter) images were obtained for calibration before initiating shadow-radiograph acquisition.

A cosmic ray filter was applied to all images to reduce data noise associated with non-neutron background radiation detection events. To further reduce anomalous noise, a total of three individual radiographs with an exposure length of 10 s for *Mesenosaurus*, 60 s for ROMVP86543 and ROMVP87043, and 15 s for *Aerosaurus* were acquired at each angle (Mays et al., 2017). These individual radiographs were summed in post-acquisition processing using the 'Grouped ZProjector' plugin in ImageJ v.1.51h (National Institutes of Health); this plugin was developed by Holly (2004). Total scan time was 14 h for *Mesenosaurus*, 42.2 h for ROMVP86543 and ROMVP87043, and 18.9 h for *Aerosaurus*.

For ROMVP86543 and ROMVP87043, neutron-induced radioactivity was measured 5 h post-irradiation by surface contact with a portal dose meter; the dose rate from both specimens was 24 μSv/h. Twelve days later, no measurable radioactivity was detectable from either specimen and both specimens were issued with a radiation clearance certificate for return.

Tomographic reconstruction of the 16-bit raw data was performed using Octopus Reconstruction v.8.8 (Inside Matters NV), yielding virtual slices perpendicular to the rotation axis. When these slices are stacked in a sequence, they form a three-dimensional volume image of the sample.

Varanodon and *Mycterosaurus* were micro-CT scanned at the University of Chicago's PaleoCT facility, at 120 kV and using a 0.2 mm Cu filter for *Varanodon* and 135 kV and a 0.5 mm Cu filter for *Mycterosaurus*. For *Varanodon*, a total of 1700 projections were taken over a total scan time of 39 min, to produce a final voxel size of 95.3 × 95.3 × 95.3 μm. For *Mycterosaurus*, a total of 1600 projections were taken over a total scan time of 3h36, producing a final voxel size of 30.3 × 30.3 × 30.3 μm.

Three-dimensional renderings of the cranial and otic endocasts were produced by manual segmentation in AVIZO Lite 9.7.0. Bony labyrinth measurements were taken following the protocol of Benoit, Manger, Fernandez, et al. (2017). Hearing range estimates were calculated using the equations of Walsh et al. (2009). Unprocessed 16-bit TIFF slices for all specimens are available online through MorphoSource (https://www.morphosource.org/projects/000387762?id=000387762&locale=en&locale=en).

Due to the isolated nature of the majority of the specimens, and incomplete preservation of the braincase of *Mesenosaurus* (only the right half of the roof is preserved, damage to the ventral surface of the braincase, and the lack of a preserved ethmoid region), the endocasts generated here are incomplete. Endocasts of the posterior portion of the braincase of all six specimens and of the anterodorsal portion of the braincase of *Mesenosaurus* are presented here, but the anteroventral portion of the endocast is absent in all specimens, and several cranial nerve foramina are not preserved. For ease of description, the reconstructed digital casts will be referred to with the same name as the soft-tissue structures they once housed (e.g. the digital cast of the hypoglossal nerve will be referred to simply as the "hypoglossal nerve").

2.3 | Institutional abbreviations

UCMP, University of California Museum of Paleontology, Berkeley, California, U.S.A.; FMNH, Field Museum of Natural History, Chicago, Illinois, U.S.A.; OMNH, Sam Noble Oklahoma Museum of Natural History, Norman, Oklahoma, U.S.A.; ROMVP, Royal Ontario Museum, Toronto, Ontario, Canada.

3 | DESCRIPTION

3.1 | Brain

The varanopid brain is tubular in shape, lacking any distinct pontine or cephalic flexures (Figures 1 and 2). The contours of the various regions of the brain (e.g. optic lobes, medulla oblongata) are difficult to discern in all specimens (i.e. the endocast in the predicted region is fairly amorphous) (Figures 1 and 2), indicating a relatively poor fit between the brain and the surrounding hard tissues, as with many non-mammalian taxa (Hopson, 1979; Schade et al., 2020). The forebrain is discernible only in *Mesenosaurus*, in which the olfactory bulbs are narrow and the olfactory tracts are highly elongated (Figures 1a, 2a).

The pituitary fossa appears to differ across specimens, but it is unclear whether this reflects a true difference or simply differences in preservation. Only the posterior half of the fossa is preserved in *Mesenosaurus*, ROMVP86543, and ROMVP87043 (Figure 2a–c); the fossa cannot be distinguished in *Mycterosaurus*, *Aerosaurus*, or *Varanodon*. In the three specimens preserving the structure, the fossa is oval in shape, and in *Mesenosaurus* and ROMVP86543 it appears contiguous with the rest of the brain. In ROMVP87043, the pituitary appears to extend further ventrally from the rest of the brain than is seen in the other two specimens.

A large recess, tentatively identified here as a floccular fossa, occupies the periotic region of all specimens except *Varanodon* (Figures 1–3), suggesting that it is a feature shared across varanopids. No fossa could be identified in *Varanodon*, but this is likely due to the quality of preservation. In the mycterosaurines, the fossa extends anteroposteriorly into the spaces defined by the anterior and posterior semicircular canals, posterolaterally to the level of the lateral semicircular canal, and ventrally to open at the fenestra vestibuli (Figures 1a-d, 2a-d). In *Aerosaurus*, the floccular fossa appears to occupy a similar position, but the full extent of the fossa could not be distinguished (Figures 1e, 2e).

3.2 | Innervations

The paths of several cranial nerves are preserved in *Mesenosaurus*, the two indeterminate mycterosaurines (ROMVP86543 and ROMVP87043), and *Aerosaurus*; innervations could not be traced in *Mycterosaurus* or *Varanodon*. The facial nerve (CN.VII) originates anterior to the vestibule and extends ventrolaterally to exit the otic capsule posteroventral to the trigeminal nerve (CN.V) (Figure 2). Langston and Reisz (1981) identified foramina for both the palatal and hyomandibular branches of the facial nerve in *Aerosaurus*; while the latter branch was successfully reconstructed in the digital endocast, the path of the former branch could not be traced in the CT data (Figure 2e). The metotic foramen (CN.X-XI) is large in all specimens (Figure 1). It is broadest at its proximal end, where it exits the brain posterior to the common crus and medial to the secondary common crus, before tapering slightly at its midlength. The foramen passes posteroventrolaterally, following the same alignment as the posteromedial surface of the secondary common crus, exiting the braincase between the opisthotic and exoccipital.

The only notable difference in cranial nerve innervation across varanopids is the difference in the relative size and positioning of the two hypoglossal foramina. In *Aerosaurus*, the larger foramen is almost directly dorsal to the smaller one, while in the mycterosaurines, the smaller foramen is positioned ventrolaterally to the larger foramen (Figure 4). Because multiple roots can emerge from a single foramen, or each root can emerge from its own foramen, the relationship between hypoglossal foramina and the actual number of hypoglossal nerve roots is not straightforward (Hopson, 1979); the presence of two foramina indicates that the varanopid hypoglossal nerve complex had at least two roots, but inferences beyond that are uncertain.

The internal carotids could only be identified in *Aerosaurus* and *Mesenosaurus* (Figure 2a,e), but their paths are incomplete in *Aerosaurus* due to damage to the specimen during preparation (Langston & Reisz, 1981). In both *Mesenosaurus* and *Aerosaurus*, the carotids enter the braincase at the posterior portion of the parasphenoid plate and pass anteriorly. In *Aerosaurus*, the canals birfucate, with the ventral branch continuing anteriorly through the parasphenoid while the dorsal branch arcs dorsally, where they would have entered the brain at the pituitary fossa. The entrance of the internal carotids into the brain could not be traced in *Mesenosaurus*.

3.3 | Canals and vestibule

In the mycterosaurines, the labyrinth is fully preserved in *Mesenosaurus*, ROMVP86543, and ROMVP87043; only fragments of the canal system in *Mycterosaurus* could be extracted, but the preserved components suggest that the morphology of *Mycterosaurus* conforms to that seen in the other three specimens. In the varanodontines, the labyrinth is fully preserved in *Aerosaurus* but could not be digitally extracted in *Varanodon*.

The varanopid inner ear is highly ossified, lacking only a fully ossified medial wall; this is a largely unexpected finding, as pelycosaur-grade synapsids have been described as having unossified internal otic capsules based on external examination of specimens (Allin & Hopson, 1992; Clack, 1997). Contrary to expectations, the paths of the semicircular canals, all three ampullae, and the vestibule are clearly defined (Figure 5). The labyrinth is housed almost entirely within the supraoccipital-opisthotic complex, with only the ventral half of the vestibule being framed by the prootic (Figure 6).

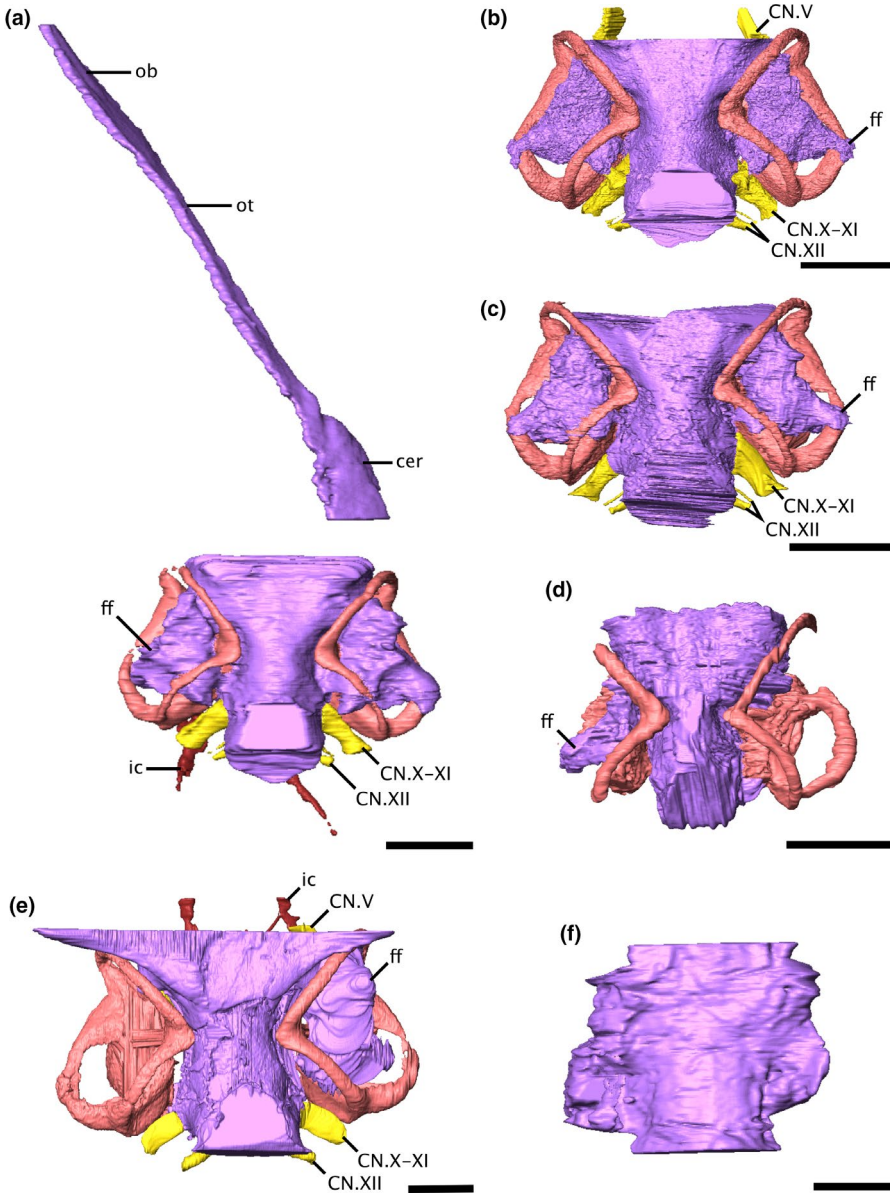

FIGURE 1 Virtual endocasts of the varanopid brain and bony labyrinth in dorsal view. (a) *Mesenosaurus*, (b) ROMVP87043, (c) ROMVP86543, (d) *Mycterosaurus*, (e) *Aerosaurus*, and (f) *Varanodon*. Due to the disarticulation of the braincase from the skull roof of *Mesenosaurus*, the anterior portion of the endocast is visible in left dorsolateral view, while the posterior portion is shown in dorsal view. Scale bars equal 5 mm. cer, cerebrum; CN.V, trigeminal nerve; CN.X-XI, metotic foramen; CN.XII, hypolossal nerve; ff, floccular fossa; ic, internal carotid artery; ob, olfactory bulbs; ot, olfactory tracts [Colour figure can be viewed at wileyonlinelibrary.com]

The common crus is curved slightly caudally, such that the anterior semicircular canal (ASC) is longer and more dorsally elevated than the posterior canal (PSC) (Figure 5). The ASC is arcuate along its entire length, whereas the PSC is almost straight in its middle portion and is anterodorsally bowed at its midsection. The ASC is the longest canal and shows the largest radius of curvature in all specimens (Table 1), but the PSC and LSC are roughly equivalent both in length and radius, with the LSC being marginally longer or showing a larger radius in *Aerosaurus* and *Mycterosaurus*, while in *Mesenosaurus*, ROMVP86543, and ROMVP87043, the PSC is marginally longer and larger.

The angles between the ASC and PSC, and between the ASC and LSC, are sub-orthogonal in all specimens (Table 1); however, the angle between the LSC and PSC is substantially more acute in the mycterosaurines, ranging from 59° to 68°, but is closer to orthogonal in *Aerosaurus*, at 81°. A secondary common crus (SCC) is visible at the intersection of the PSC and LSC, but the paths of the individual canals through the SCC can still be traced (Figure 5); the arc of the PSC passes ventrally to the LSC, which in turn curves toward the vestibule medial to the duct of the PSC.

The anterior and lateral ampullae are prominent in *Mesenosaurus*, ROMVP86543, ROMVP87043, and *Aerosaurus* (Figure 5). As the ventral arm of the PSC and the posterior arm of the LSC are fused into a secondary common crus, both canals share the entrance into the posterior ampulla. The posterior canal enters the vestibule just ventral to the lateral canal, within the posterior ampulla.

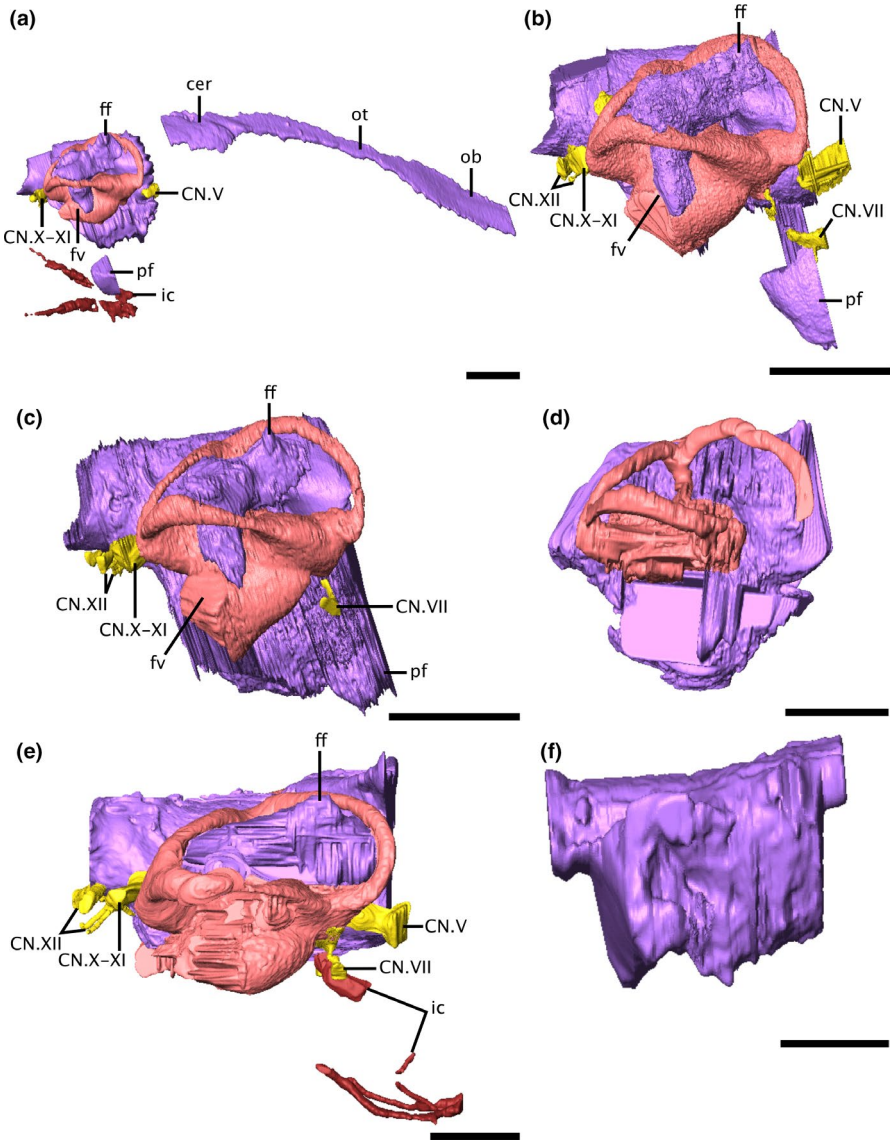

FIGURE 2 Virtual endocasts of the varanopid brain and bony labyrinth in right lateral view. (a) *Mesenosaurus*, (b) ROMVP87043, (c) ROMVP86543, (d) *Mycterosaurus*, (e) *Aerosaurus*, (f) *Varanodon*. Due to the disarticulation of the braincase from the skull roof of *Mesenosaurus*, the anterior portion of the endocast is visible in right dorsolateral view, while the posterior portion is shown in right lateral view. Scale bars equal 5 mm. cer, cerebrum; CN.V, trigeminal nerve; CN.VII, facial nerve; CN.X-XI, metotic foramen; CN.XII, hypolossal nerve; ff, floccular fossa; ic, internal carotid artery; ob, olfactory bulbs; ot, olfactory tracts; pf, pituitary fossa [Colour figure can be viewed at wileyonlinelibrary.com]

The vestibule is not distinguishable in *Mycterosaurus* or *Varanodon*; in the four specimens in which it is preserved, it is large, oval, and posteroventrally inclined (Figure 5). There is no indication of separation of the utricular and saccular regions of the vestibule, nor is there a distinct cochlear recess. The fenestra vestibuli is positioned at the posteroventralmost point of the vestibule and appears to communicate directly with the external surface of the skull. The hearing range and mean best hearing frequency, estimated from the length of the vestibule, are low, ranging between 2400–4800 Hz and 1500–2800 Hz, respectively.

The most noticeable difference in the morphology of the inner ear between the mycterosaurines and the varanodontines is the difference in relative canal system height. The canal system is dorsoventrally shorter and more anteriorly elongated in *Aerosaurus* (Figure 5u), such that the ASC follows a more oval curvature, extending farther anteriorly from the anterior ampulla, rather than arcing directly dorsally as in the mycterosaurines (Figure 5).

4 | DISCUSSION

4.1 | Phylogenetic considerations

ROMVP86543 and ROMVP87043 were identified as varanopids due to the tall, narrow paroccipital processes, which have been identified as synapomorphic for varanopids (Campione & Reisz, 2010), and due to the overall morphological similarity between ROMVP86543,

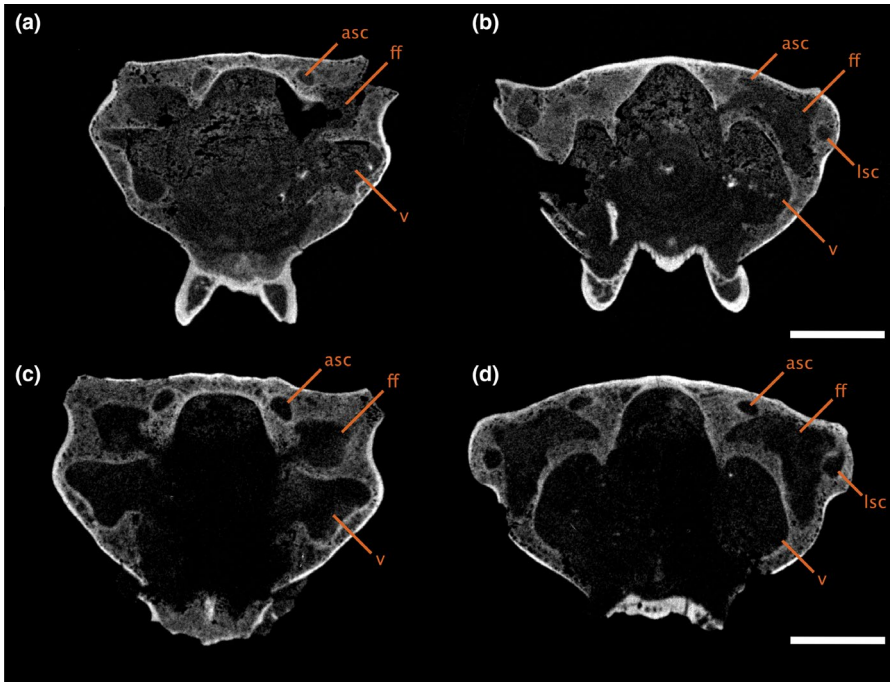

FIGURE 3 Transverse CT slices through the braincase of (a-b) ROMVP86543 and (c-d) ROMVP87043, showing the shape and position of the floccular fossa, moving anteroposteriorly with A,C anterior to the common crus and B,D posterior to the common crus. Scale bars equal 5 mm. asc, anterior semicircular canal; ff, floccular fossa; lsc, lateral semicircular canal; psc, posterior semicircular canal; v, vestibule [Colour figure can be viewed at wileyonlinelibrary.com]

ROMVP87043, and the braincase of OMNH 73209 which is known to be a mycterosaurine varanopid (*Mesenosaurus efremovi* Maho et al., 2019). ROMVP86543 and ROMVP87043 are identical to the braincase of *Mesenosaurus* with the single exception of the ventral surface of the parasphenoid plate, discussed below.

The morphology of the paroccipital processes indicates a probable mycterosaurine identity for ROMVP86543 and ROMVP87043; although the processes are broken on both specimens, the preserved proximal ends suggest a similar anteroposteriorly-oriented oval cross-section as in other mycterosaurines (Figure 7), including *Mesenosaurus* (Maho et al., 2019; Reisz & Berman, 2001), rather than the broad, blade-like process of the varanodontines (Langston & Reisz, 1981). However, the placement of ROMVP86543 and ROMVP87043 within Mycterosaurinae remains uncertain, as the diagnostic criteria for *Mesenosaurus* and *Mycterosaurus* do not include any braincase characters other than the stapes, which is not preserved for either ROMVP86543 or ROMVP87043 (Berman & Reisz, 1982; Maho et al., 2019). Nonetheless, the morphology of the parasphenoid plate suggests that they are likely neither *Mesenosaurus* nor *Mycterosaurus*, as they exhibit a low median ridge flanked by two depressions, in contrast to the single median depression seen in the latter two genera (Berman & Reisz, 1982; Maho et al., 2019) (Figure 8). A similar ridge has been described in the varanopid '*Basicranodon*' (Vaughn, 1958; but see Maho et al., 2019 for discussion of the validity of the taxon). A more exact determination of the placement of ROMVP86543 and ROMVP87043 within the mycterosaurines will depend upon the description of more complete specimens with diagnostic characters.

4.2 | Comparisons with other Palaeozoic amniotes

Here we provide a brief comparative discussion of our findings with those of previous works on other Palaeozoic amniotes. Comparisons with other pelycosaur-grade synapsid taxa are precluded by the overall lack of endocast data; as such, comparisons here are by necessity limited to Permian therapsids, with reference to captorhinids where possible and to extant taxa where necessary. Table 2 provides a brief summary of some key differences in selected traits across taxa.

4.2.1 | Brain

Compared with more derived synapsids, the varanopid brain is largely plesiomorphic in most aspects, being tubular and showing no enlargement of the cerebellum, cerebrum, or olfactory bulbs, nor any division of the cerebrum into two hemispheres. Most non-mammalian therapsid endocasts are similar, being limited to a long tubular endocast with minimal differentiation of the different brain regions and only slight flexion at most (Araújo et al., 2017; Bendel et al., 2018; Benoit, Manger, Norton et al., 2017; Castanhinha et al., 2013; Laaß, 2015a). Exceptions to this include the biarmosuchians, in which the cranial endocast displays a very strong flexure, such that the forebrain is horizontal while the hindbrain is nearly vertical (Benoit, Fernandez, et al., 2017), and potentially *Dimetrodon*, although the degree of flexure shown by *Dimetrodon* is not agreed upon (Case, 1907; Hopson, 1979).

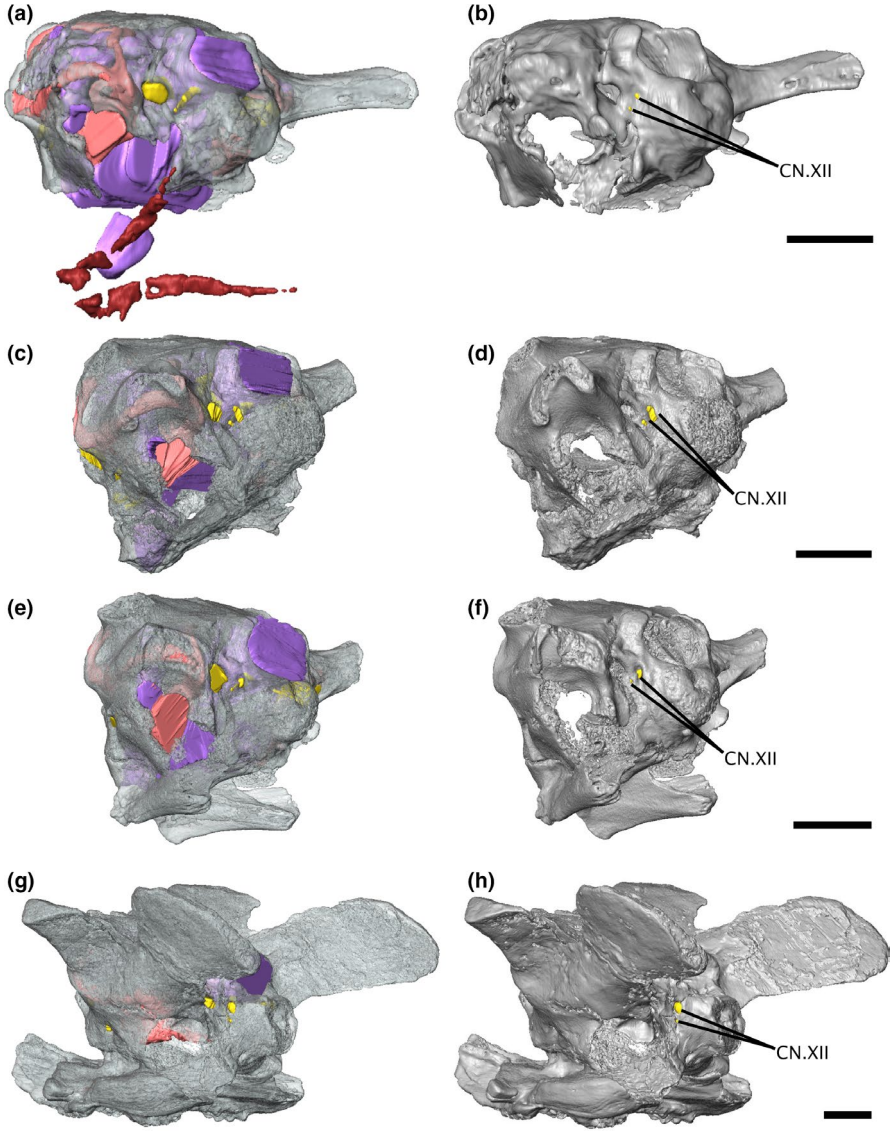

FIGURE 4 Isosurface renderings of the varanopid braincase in left posterolateral view, showing the relative positioning of the hypoglossal foramina. (a-b) *Mesenosaurus*, (c-d) ROMVP87043, (e-f) ROMVP86543, (g-h) *Aerosaurus*. Scale bars equal 5 mm. CN.XII, hypoglossal nerve [Colour figure can be viewed at wileyonlinelibrary.com]

The presence of a putative floccular fossa in all but the most poorly preserved specimen suggests that enlarged floccular fossae are a feature shared across varanopids. The floccular fossa is only slightly enlarged in the biarmosuchians, anomodonts, and gorgonopsians, and is very shallow in the dinocephalians (Araújo et al., 2017, 2018; Bendel et al., 2018; Benoit, Fernandez, et al., 2017; Benoit, Manger, Fernandez, et al., 2017; Laaß, 2015a). Structures such as these are frequently identified as floccular fossae in fossil taxa (e.g., Schade et al., 2020), on the assumption that they contained the flocculus in life; however, this fossa is known to house different neural tissues in various extant groups and the size relationship between the fossa and the flocculus itself is not precise, such that the relationship between floccular fossa size and behaviour is not straightforward (Schade et al., 2020). Despite this, large floccular fossae are frequently interpreted as indicative of a high degree of head-eye coordination, as the flocculus is heavily involved in gaze stabilization and reflex control of the neck (De Zeeuw & Koekkoek, 1997; Spoor et al., 2007; Walsh et al., 2013; Witmer et al., 2003). If the identification of this structure as a floccular fossa is correct, the extremely large size of the fossa may indicate that varanopids possessed highly developed head-eye coordination, which would align with their large orbits and their inferred predatory feeding mode (Reisz & Modesto, 2007).

4.2.2 | Canals and vestibule

The varanopid bony labyrinth shares many features with more derived synapsids, including a distinct secondary common crus and a partly unossified medial wall (Benoit, Manger, Fernandez, et al., 2017). In most non-mammalian therapsids, the medial walls of the vestibule, common crus, ampullae, and anterior and lateral canals are

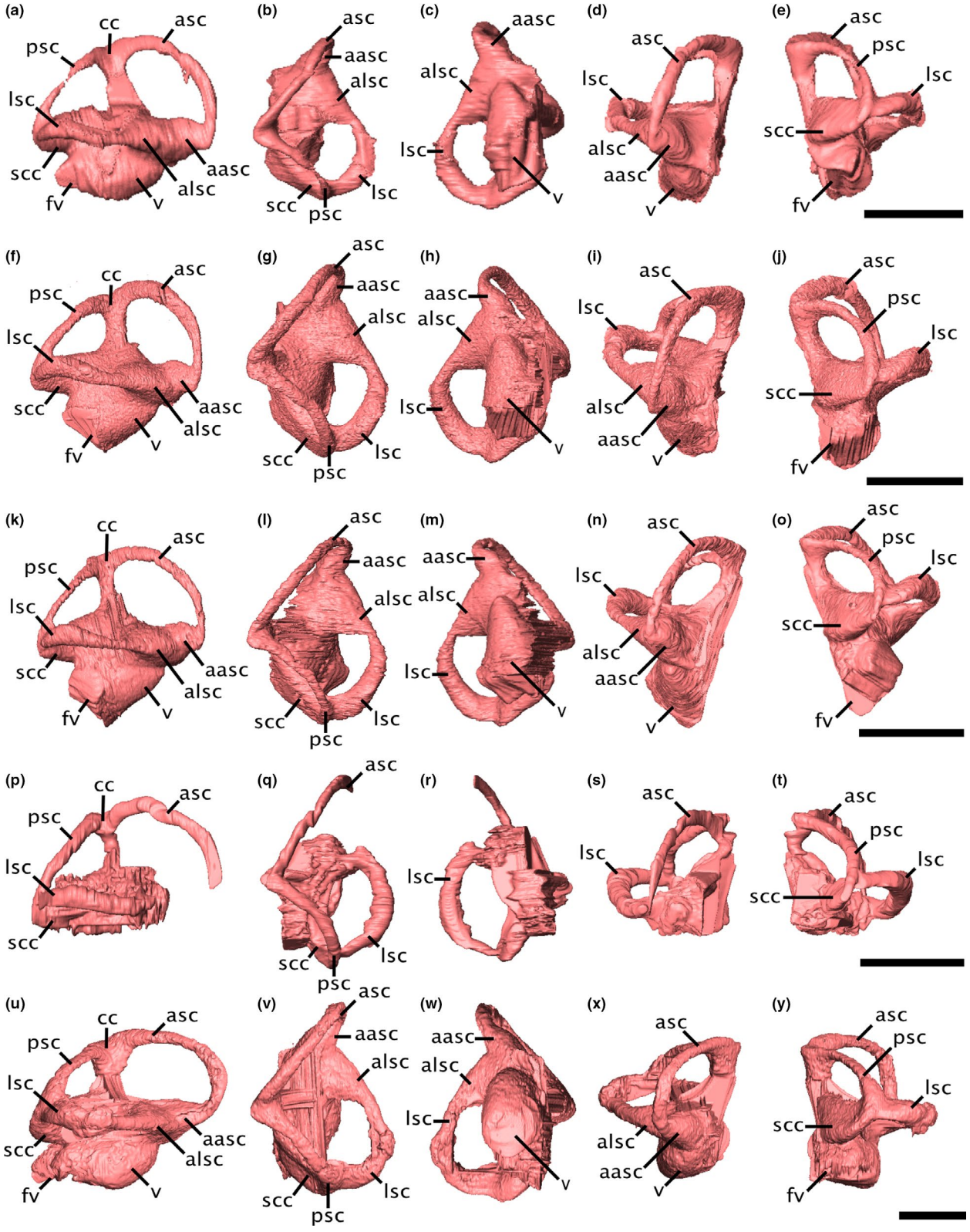

FIGURE 5 Virtual endocasts of the varanopid bony labyrinth. (a-e) *Mesenosaurus*, (f-j) ROMVP87043, (k-o) ROMVP86543, (p-t) *Mycterosaurus*, (u-y) *Aerosaurus* in (a,f,k,p,u) right lateral, (b,g,l,q,v) dorsal, (c,h,m,r,w) ventral, (d,i,n,s,x) anterior, and (e,j,o,t,y) posterior views. Scale bars equal 5 mm. aasc, ampulla of the anterior semicircular canal; alsc, ampullae of the lateral semicircular canal; asc, anterior semicircular canal; fv, fenestra vestibuli; lsc, lateral semicircular canal; psc, posterior semicircular canal; scc, secondary common crus; v, vestibule [Colour figure can be viewed at wileyonlinelibrary.com]

unossified (Benoit, Manger, Norton, et al., 2017; Castanhinha et al., 2013; Ivakhnenko, 2008; Laaß, 2016; Luo, 2001), with biarmosuchians displaying a seemingly derived state of being much more fully encapsulated (Benoit, Manger, Fernandez, et al., 2017). Interestingly, the biarmosuchian condition is more similar to that seen in the varanopids described here, where the only unossified regions of the medial wall are those of the vestibule and a small portion of the common crus and anterior ampulla. As biarmosuchians represent the basalmost clade of therapsids (Liu et al., 2009; Rubidge & Sidor, 2001), this similarity with the much earlier-diverging varanopids suggests that the reduced ossification of the medial wall in other non-mammalian therapsids may be a derived condition, with the higher degree of ossification in the varanopids and biarmosuchians possibly representing the plesiomorphic state.

The relative contributions of the prootic, opisthotic, and supraoccipital to the housing of the bony labyrinth appear to differ strongly in varanopids from that seen in other Permian amniotes. In the dinocephalian *Anteosaurus*, the ASC, lateral ampulla, and the anterior portion of the vestibule are bordered by the prootic, while the PSC and the posterior portion of the LSC are bordered by the opisthotic (Benoit, Kruger, et al., 2021). In the therocephalian *Lycosuchus*, the labyrinth is housed by not only the prootic, opisthotic, and supraoccipital, but also the basioccipital and exoccipital (Pusch et al., 2020). The captorhinid canal system is encapsulated by the prootic, opisthotic, and supraoccipital, with the prootic housing the anterior and lateral ampullae and the anterior half of the LSC and the opisthotic housing the posterior ampulla, the posterior half of the LSC, and the lagena (Heaton, 1979).

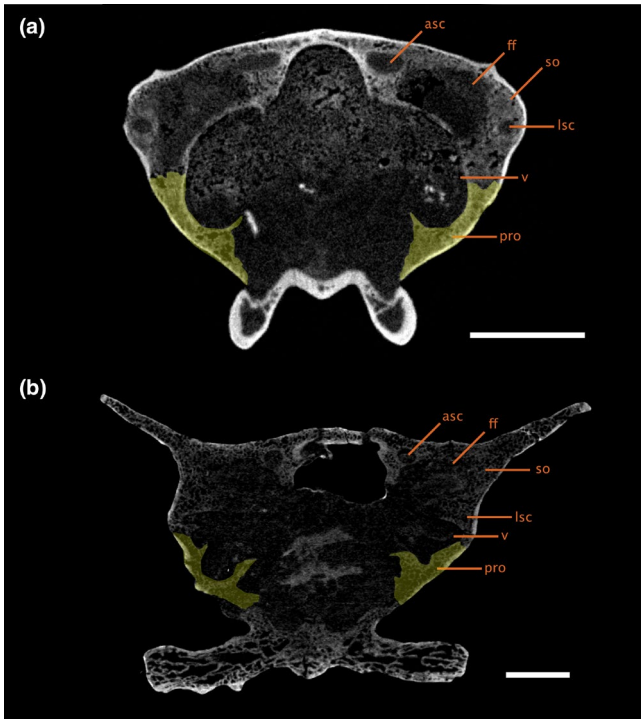

FIGURE 6 Transverse CT slice through the braincase of (a) ROMVP86543 and (b) *Aerosaurus*, showing the positioning of the bony labyrinth within the braincase. The left prootic is indicated in yellow. Scale bars equal 5 mm. asc, anterior semicircular canal; ff, floccular fossa; lsc, lateral semicircular canal; pro, prootic; so, supraoccipital-opisthotic complex; v, vestibule [Colour figure can be viewed at wileyonlinelibrary.com]

The dorsal expansion of the anterior semicircular canal, as shown by the posterior tilt of the common crus, is very slight in varanopids, in contrast to that shown by a number of biarmosuchians, therocephalians, and gorgonopsians (Araújo et al., 2017; Benoit, Manger, Fernandez, et al., 2017). The varanopid lateral canal shows a slight degree of non-planarity, similar to that seen in the therocephalians *Euchambersia* and *Microgomphodon* (Benoit, Manger, Fernandez, et al., 2017). However, this deviation from planarity is slight, even in contrast with the strongly planar canals of the biarmosuchians (Benoit, Manger, Fernandez, et al., 2017); the functional implications of non-planarity are unclear, even in taxa with substantially greater deviations from planarity (Ekdale, 2013), so we do not attempt any functional interpretations here.

The anterior semicircular canal is largest, both in length and radius, in numerous crown amniotes including mammals and non-mammalian therapsids (Benoit, Manger, Fernandez, et al., 2017), squamates (Yi & Norell, 2019), and archosaurs (Georgi et al., 2013), and this pattern holds within varanopids as well. Semicircular canal size is thought to be correlated with head mobility and agility in tetrapods (e.g., Clarke, 2005; Georgi et al., 2013; Spoor et al., 2002; Stokstad, 2003), and as such the enlargement of the anterior canal should serve as an indication of a greater degree of vertical mobility of the head (Clarke, 2005). However, as Benoit, Manger, Fernandez, et al., (2017) noted, taxa possessing similarly enlarged anterior canals can vary substantially in both body mass and bony labyrinth orientation, the latter being potentially indicative of differences in head posture (but see Benoit et al., 2020), so it is questionable whether anterior canal enlargement is solely, or even largely, due to similarities in the movement of the head.

The varanopid vertical canals are strongly elliptical, more like those of extant squamates than extant mammals (Araújo et al., 2018; Goyens, 2019). Both the degree of eccentricity shown by the varanopid vertical canals and the near-orthogonality of all three canals are similar to that seen in the dicynodonts *Endothiodon* and *Niassodon* (Araújo et al., 2018). Araújo et al. (2018) suggest that the combination of high ellipticity and orthogonality is indicative of specialization for rapid head movements; as with many functional arguments regarding semicircular canal morphology, the presence and degree of a relationship between high ellipticity and/or high orthogonality and canal sensitivity or movement specialization is not universally agreed upon (Ekdale, 2013; Grohé et al., 2016; Maddin & Sherratt, 2014; Vasilopoulou-Kampitsi et al., 2019). Nonetheless, if such a relationship does exist, the presence of strongly elliptical and orthogonal canals in varanopids, in combination with the enlarged floccular fossae, would lend further support to their inferred predatory feeding mode.

The varanopid vestibule is short and rounded, in contrast to the substantially more elongated vestibule of therapsids including gorgonopsians and biarmosuchians (Bendel et al., 2018; Benoit, Manger, Fernandez, et al., 2017). Until recently, a distinct cochlear recess was

TABLE 1 Measurements of the bony labyrinth and estimation of the hearing range and best hearing frequency of the varanopids studied

	Mesenosaurus	*Mycterosaurus*	ROMVP86543	ROMVP87043	*Aerosaurus*
Basicranial length (mm)	15.90	--	8.86	11.60	24.39
Vestibule length (mm)	3.00	--	3.77	2.99	4.25
Labyrinth length (mm)	7.96	--	8.84	8.86	11.25
ASC height (mm)	4.16	3.75	3.86	4.35	4.87
ASC width (mm)	5.34	5.51	5.43	5.57	8.16
ASC length (mm)	9.19	8.77	9.13	9.85	13.53
ASC radius of curvature (mm)	2.37	2.31	2.32	2.48	3.26
ASC eccentricity	0.73	0.82	0.80	0.81	0.80
PSC height (mm)	2.74	2.29	2.28	2.75	3.02
PSC width (mm)	4.61	4.02	4.37	4.56	6.28
PSC length (mm)	6.62	5.59	5.77	6.51	7.16
PSC radius of curvature (mm)	1.84	1.58	1.66	1.83	2.33
PSC eccentricity	0.88	0.90	0.90	0.87	0.88
LSC height (mm)	3.21	2.95	2.98	3.21	4.45
LSC width (mm)	4.67	4.87	4.29	4.94	6.13
LSC length (mm)	5.02	6.39	5.28	5.96	8.54
LSC radius of curvature (mm)	1.97	1.95	1.82	2.04	2.64
LSC eccentricity	0.42	0.65	0.53	0.49	0.57
Hearing range (Hz)	2545.15	---	4806.60	3536.05	2398.67
Mean best hearing frequency (Hz)	1597.70	---	2824.44	2135.22	1518.25
∠ ASC-PSC (°)	85	93	84	87	90
∠ ASC-LSC (°)	87	88	89	85	96
∠ PSC-LSC (°)	68	68	63	59	81

Note: Measurements are averaged from both labyrinths, except in *Mycterosaurus*, where only the right labyrinth can be seen.

only known in non-mammalian cynodonts, but possible recesses have been identified in the biarmosuchian *Lemurosaurus*, the therocephalian *Microgomphodon*, and the dicynodonts *Niassodon* and *Pristerodon* (Benoit, Manger, Fernandez, et al., 2017; Castanhinha et al., 2013; Laaß, 2015a, 2016). The lack of an identifiable cochlear recess in any of the specimens described here supports the hypothesis that distinct recesses only arose within Therapsida. However, as has been noted elsewhere (Benoit, Manger, Fernandez, et al., 2017), it is important to distinguish between a lack of a distinct cochlear recess and the absence of a basilar papilla; work by Fritzsch et al. (2013) has argued that the presence of a basilar papilla may be the ancestral condition for all tetrapods, and other vertebrates such as sarcopterygian fishes are known to have small basilar papilla that are not reflected in the morphology of the bony labyrinth (Fritsch, 1987; Manley, 2012).

4.3 | Phylogenetic implications

Palaeoneurological information appears to be highly informative in discussions of the placement of varanopids within amniotes (Benoit, Ford, et al., 2021). The morphology of the maxillary canal supports their position as basal synapsids, being similar to that of other pelycosaur-grade synapsids and more derived therapsids including dicynodonts and therocephalians, and different from that of basal sauropsids (Benoit, Ford, et al., 2021). At least some palaeoneurological characters are known to be fairly conserved across synapsids (such as the maxillary canal; Benoit, Ford, et al., 2021); in line with this, the morphology of the inner ear is also known to carry a phylogenetic signal, although the relative strength of the effect of phylogeny, as opposed to that of ecology, is unclear (e.g., Benson et al., 2017; Ekdale, 2016; Palci et al., 2017).

The high degree of ossification of the varanopid inner ear is much more similar to that seen in other synapsids, in contrast to the largely unossified condition seen in basal sauropsids (Gardner et al., 2010). Similarly highly ossified labyrinths are known from all members of the synapsid lineage for which an endocast of the inner ear has been described (e.g., Benoit, Fernandez, et al., 2017; Benoit, Manger, Fernandez, et al., 2017; Benoit, Manger, Norton et al., 2017; Castanhinha et al., 2013; Day et al., 2018; Laaß, 2015a). The late Permian diapsid *Youngina* is the earliest sauropsid with a described otic endocast, and displays a minimal degree of internal ossification within the otic capsule (Gardner et al., 2010); within sauropsids, highly ossified capsules with clear differentiation of all inner ear components

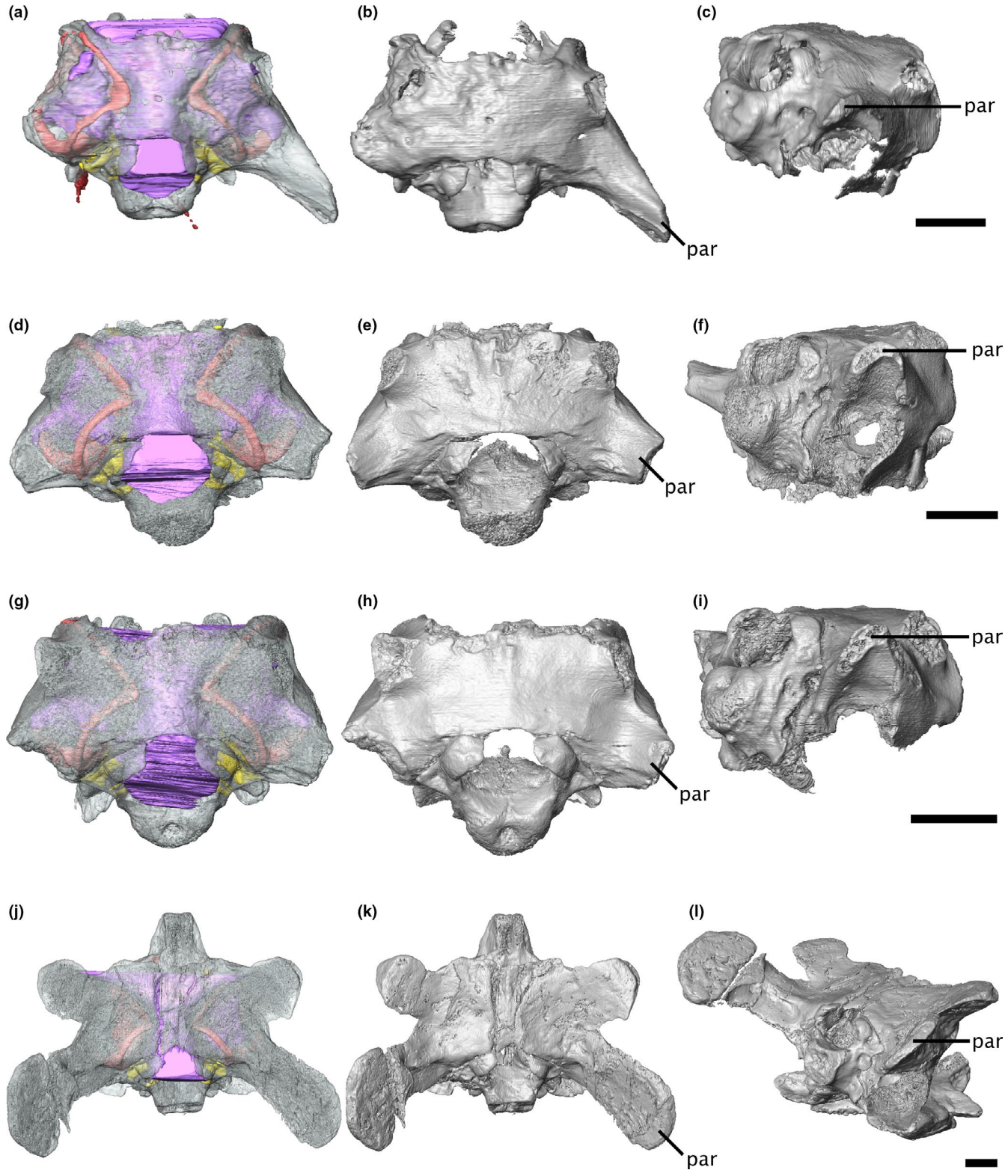

FIGURE 7 Isosurface renderings of the varanopid braincase, showing differences between mycterosaurine and varanodontine paroccipital processes. (a-c) *Mesenosaurus*, (d-f) ROMVP87043, (g-i) ROMVP86543, and (j-l) *Aerosaurus* in (a-b, d-e, g-h, j-k) dorsal and (c, f, i, l) right posterodorsolateral view. Scale bars equal 5 mm. par, paroccipital process [Colour figure can be viewed at wileyonlinelibrary.com]

only seem to arise in more derived members (e.g., Neenan & Scheyer, 2012; Sobral & Müller, 2019; Sobral et al., 2016).

Comparative endocast data on a broad range of Palaeozoic amniotes will be required in order to thoroughly test the implications of palaeoneurological characters for the placement of varanopids within amniotes. The tetrapod braincase has been demonstrated to preserve phylogenetic indicators that are obscured in other, more evolutionarily labile regions of the skull (Cardini & Elton, 2008; Lieberman et al.,

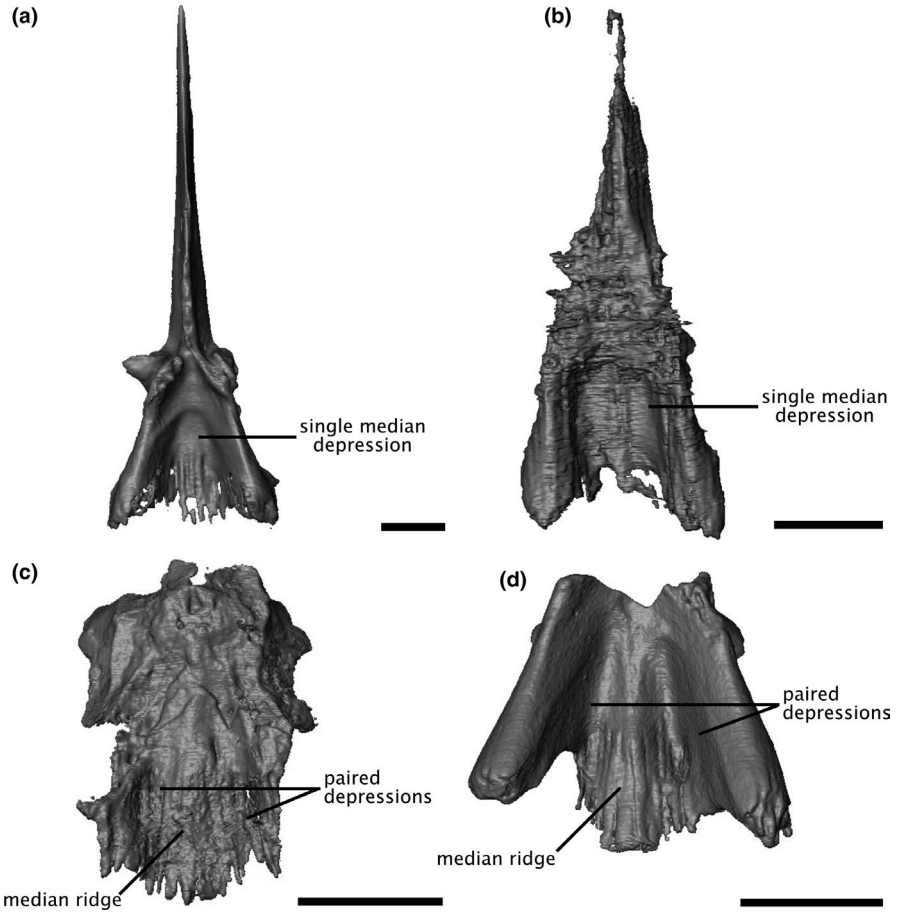

FIGURE 8 Digital renderings of the mycterosaurine parasphenoid in ventral view. (a) *Mesenosaurus*, (b) *Mycterosaurus*, (c) ROMVP87043, (d) ROMVP86543. Scale bars equal 5 mm

TABLE 2 Comparison of various palaeoneurological traits in selected Palaeozoic amniotes

	Varanopidae	Biarmosuchia	Dinocephalia	Anomodontia	Gorgonopsia	*Youngina*
Pontine flexure	None	Strong	Strong	Slight	Slight	---
Cephalic flexure	None	Strong	Slight	Slight	Slight	---
Olfactory tracts	Long	Long	Short	Short	Short	---
Flocculus	Large	Moderate	Small	Moderate	Moderate	---
Medial wall of otic capsule	Mostly ossified	Mostly ossified	Mostly ossified	Partly ossified	Partly ossified	Unossified
Vestibule	Short, round	Short, thin	Long, straight	Long, curved	Long, straight	Short, straight
Cochlear recess	None	Putative	None	None	None	None
Ampullae	Prominent	Prominent	Inconspicuous	Inconspicuous	Inconspicuous	Inconspicuous

Note: Dashed lines indicate taxa whose states are unknown or undescribed for a given trait. Traits for varanopids are described here; traits for other clades are from Gardner et al. (2010), Laaß (2015a), Benoit et al. (2017a-c), Araújo et al. (2017, 2018), and Bendel et al. (2018).

2000; Maddin et al., 2012); as such, endocranial information presents a potentially rich new dataset of characters than can help to resolve the position of varanopids, among many other phylogenetic questions.

4.4 | Functional inferences

The varanopid vestibule is very short, contrasting markedly with the elongated vestibules of more derived synapsids (Araújo et al., 2017, 2018; Bendel et al., 2018; Benoit, Manger, Norton, et al., 2017; Laaß, 2015a). The length of the vestibule has been shown to provide a proxy for estimating hearing frequency sensitivity, with longer vestibules being associated with a greater sensitivity to higher frequencies (Walsh et al., 2009). Elongation of the vestibule, and thus higher-frequency hearing sensitivity, is thought to be associated in some taxa with the evolution of active predatory behaviours, as it provides an advantage for detecting and catching prey (Choiniere et al., 2021). Similarly, a shortening of vestibule length

(and thus a reduction of higher-frequency hearing sensitivity) has been shown in some lineages that evolve herbivorous behaviours (Choiniere et al., 2021).

Perhaps unsurprisingly, given the extremely short vestibular length, the estimated hearing sensitivity of varanopids is very low, ranging from 1500–2800 Hz mean best hearing frequency (Table 1), in contrast to more derived synapsids which range from 4000–5700 Hz (Benoit Manger, Fernandez, et al., 2017). This suggests that, despite gaining some of the predatory features seen in derived amniotes, including the highly specialized dentition and greatly enlarged floccular fossa, varanopids retain the lower-frequency hearing condition that is likely the plesiomorphic state for amniotes.

5 | CONCLUSION

This study represents the first tomographic study of the brain and bony labyrinth of any pelycosaur-grade synapsid, and the new data described here reveal aspects of varanopid neuroanatomy that have previously gone unrecognized or undescribed. The identification of a large floccular fossa, in combination with elliptical and orthogonal vertical semicircular canals, lends neuroanatomical support to prior inferences regarding the predatory feeding mode of varanopids. As recent work by Benoit, Ford et al. (2021) has shown, the use of CT to study palaeoneurological features has great relevance beyond purely morphological investigations, as it can be used to test phylogenetic hypotheses that have been derived from datasets lacking palaeoneurological characters. The morphology of the varanopid inner ear and its similarity with that of therapsids support their placement as synapsids, while revealing that varanopids retain far more plesiomorphic sensory capabilities than the later therapsids. The data described here extend our understanding of synapsid palaeoneurology to a group whose neuroanatomy has gone largely unstudied and lay the foundation for future work on pelycosaurian neuroanatomy and relationships.

ACKNOWLEDGEMENTS

Thanks to Kevin Seymour (ROMVP) for assistance with collection numbers. Thanks to the Field Museum in Chicago for providing the raw data of *Varanodon* and *Mycterosaurus*. Thanks to the University of California Museum of Paleontology for access to the isolated braincase of *Aerosaurus*. Thanks to Mary Silcox and Devin Ward for assistance with bony labyrinth skeletonization and measurement protocols. This study was supported by a Natural Sciences and Engineering Research Council (NSERC) scholarship to KDB, NSERC grants to RRR and DCE, and the generous support of the Australian Nuclear Science and Technology Organisation. The authors declare that there are no competing interests.

AUTHOR CONTRIBUTIONS

KDB: designed project, analysed and interpreted data, wrote manuscript, created figures. DCE: designed project, edited manuscript. RRR: designed project, edited manuscript. JJB: collected scan data, wrote scanning portion of Methods section. All authors approved of this article.

OPEN RESEARCH BADGES

This article has earned an Open Data and Open Materials badges for making publicly available the digitally-shareable data necessary to reproduce the reported results. The data is available at https://www.morphosource.org/projects/000387762?.

DATA AVAILABILITY STATEMENT

Unprocessed 16-bit TIFF slices for all specimens are available online through MorphoSource (https://www.morphosource.org/projects/000387762?id=000387762&locale=en&locale=en).

ORCID

Kayla D. Bazzana https://orcid.org/0000-0002-9982-6210
David C. Evans https://orcid.org/0000-0001-9608-6635

REFERENCES

Allin, E.F. (1975) Evolution of the mammalian middle ear. *Journal of Morphology*, 147, 403–438.

Allin, E.F. & Hopson, J.A. (1992) Evolution of the auditory system in Synapsida ("mammal-like reptiles" and primitive mammals) as seen in the fossil record. In: Webster, D.B., Fay, R.R. & Popper, A.N. (Eds.) *The evolutionary biology of hearing*. New York: United States of America, Springer, pp. 587–614.

Araújo, R., Fernandez, V., Polcyn, M.J., Fröbisch, J. & Martins, R.M.S. (2017) Aspects of gorgonopsian paleobiology and evolution: insights from the basicranium, occiput, osseous labyrinth, vasculature, and neuroanatomy. *PeerJ*, 5, e3119.

Araújo, R., Fernandez, V., Rabbitt, R.D., Ekdale, E.G., Antunes, M.T., Castanhinha, R. et al. (2018) *Endothiodon* cf. *bathystoma* (Synapsida: Dicynodontia) bony labyrinth anatomy, variation and body mass estimates. *PLoS One*, 13, e0189883.

Bendel, E.-M., Kammerer, C.F., Kardjilov, N., Fernandez, V. & Fröbisch, J. (2018) Cranial anatomy of the gorgonopsian *Cynariops robustus* based on CT-reconstruction. *PLoS One*, 13, e0207367.

Benoit, J., Adnet, S., El Mabrouk, E., Khayati, H., Ben Haj Ali, M., Marivaux, L. et al. (2013a) Cranial remain from Tunisia provides new clues for the origin and evolution of Sirenia (Mammalia, Afrotheria) in Africa. *PLoS One*, 8, e54307.

Benoit, J., Fernandez, V., Manger, P.R. & Rubidge, B.S. (2017a) Endocranial casts of pre-mammalian therapsids reveal an unexpected neurological diversity at the deep evolutionary root of mammals. *Brain, Behavior and Evolution*, 90, 311–333.

Benoit, J., Ford, D.P., Miyamae, J.A. & Ruf, I. (2021b) Can maxillary canal morphology inform varanopid phylogenetic affinities? *Acta Palaeontologica Polonica*, 66, 389–393.

Benoit, J., Kruger, A., Jirah, S., Fernandez, V. & Rubidge, B.S. (2021a) Palaeoneurology and palaeobiology of the dinocephalian therapsid *Anteosaurus magnificus*. *Acta Palaeontologica Polonica*, 66, 29–39.

Benoit, J., Legendre, L.J., Farke, A.A., Neenan, J.M., Mennecart, B., Costeur, L. et al. (2020) A test of the lateral semicircular canal correlation to head posture, diet and other biological traits in "ungulate" mammals. *Scientific Reports*, 10, 19602.

Benoit, J., Mabrouk, E.E., Lebrun, R., Tabuce, R. & Marivaux, L. (2013b) New insights into the ear region anatomy and cranial blood supply of stem Strepsirhini: evidence from three primate petrosals from

the Eocene of Chambi, Tunisia. *Journal of Human Evolution*, 65, 551–572.
Benoit, J., Manger, P.R., Fernandez, V. & Rubidge, B.S. (2017b) The bony labyrinth of late Permian Biarmosuchia: palaeobiology and diversity in non-mammalian Therapsida. *Palaeontologia Africana*, 52, 58–77.
Benoit, J., Manger, P.R., Norton, L., Fernandez, V. & Rubidge, B.S. (2017c) Synchrotron scanning reveals the palaeoneurology of the head-butting *Moschops capensis* (Therapsida, Dinocephalia). *PeerJ*, 5, e3496.
Benoit, J., Merigeaud, S. & Tabuce, R. (2013c) Homoplasy in the ear region of Tethytheria and the systematic position of Embrithopoda (Mammalia, Afrotheria). *Geobios*, 46, 357–370.
Benson, R.B.J., Starmer-Jones, E., Close, R.A. & Walsh, S.A. (2017) Comparative analysis of vestibular ecomorphology in birds. *Journal of Anatomy*, 231, 990–1018.
Berman, D.S. & Reisz, R.R. (1982) Restudy of *Mycterosaurus longiceps* (Reptilia, Pelycosauria) from the Lower Permian of Texas. *Annals of Carnegie Museum*, 51, 423–453.
Campione, N.E. & Reisz, R.R. (2010) *Varanops brevirostris* (Eupelycosauria: Varanopidae) from the Lower Permian of Texas, with discussion of varanopid morphology and interrelationships. *Journal of Vertebrate Paleontology*, 30, 724–746.
Cardini, A. & Elton, S. (2008) Does the skull carry phylogenetic signal? Evolution and modularity in the guenons. *Biological Journal of the Linnean Society*, 93, 813–834.
Case, E.C. (1907) Revision of the Pelycosauria of North America. *Carnegie Institute of Washington Publications*, 55, 1–176.
Castanhinha, R., Ara Jo, R., Nior, L.C., Angielczyk, K.D., Martins, G.G., Martins, R.M.S. et al. (2013) Bringing dicynodonts back to life: paleobiology and anatomy of a new emydopoid genus from the Upper Permian of Mozambique. *PLoS One*, 8, e80974.
Choiniere, J.N., Neenan, J.M., Schmitz, L., Ford, D.P., Chapelle, K.E.J., Balanoff, A.M. et al. (2021) Evolution of vision and hearing modalities in theropod dinosaurs. *Science*, 372, 610–613.
Clack, J.A. (1997) The evolution of tetrapod ears and the fossil record. *Brain, Behavior and Evolution*, 50, 198–212.
Clarke, A.H. (2005) On the vestibular labyrinth of *Brachiosaurus brancai*. *Journal of Vestibular Research*, 15, 65–71.
Conroy, G.C. & Vanier, M.W. (1984) Noninvasive three-dimensional computer imaging of matrix-filled fossil skulls by high-resolution computed tomography. *Science*, 226, 456–458.
Day, M.O., Smith, R.M.H., Benoit, J., Fernandez, V. & Rubidge, B.S. (2018) A new species of burnetiid (Therapsida, Burnetiamorpha) from the early Wuchiapingian of South Africa and implications for the evolutionary ecology of the family Burnetiidae. *Papers in Palaeontology*, 4, 453–475.
De Zeeuw, C.I. & Koekkoek, S.K.E. (1997) Signal processing in the C2 module of the flocculus and its role in head movement control. *Progressive Brain Research*, 114, 229–321.
Ekdale, E.G. (2013) Comparative anatomy of the bony labyrinth (inner ear) of placental mammals. *PLoS One*, 8, e66624.
Ekdale, E.G. (2016) Morphological variation among the inner ears of extinct and extant baleen whales (Cetacea: Mysteceti). *Journal of Morphology*, 277, 1599–1615.
Evans, D.C., Ridgely, R. & Witmer, L.M. (2009) Endocranial anatomy of lambeosaurine hadrosaurids (Dinosauria: Ornithischia): a sensorineural perspective on cranial crest function. *The Anatomical Record*, 292, 1315–1337.
Ford, D.P. & Benson, R.B.J. (2020) The phylogeny of early amniotes and the affinities of Parareptilia and Varanopidae. *Nature Ecology and Evolution*, 4, 57–65.
Fritzsch, B. (1987) The inner ear of the coelacanth fish *Latimeria* has tetrapod affinities. *Nature*, 327, 153–154.
Fritzsch, B., Pan, N., Jahan, I., Duncan, J.S., Kopecky, B.J., Elliott, K.L. et al. (2013) Evolution and development of the tetrapod auditory system: an organ of Corti-centric perspective. *Evolution and Development*, 15, 63–79.
Garbe, U., Randall, T., Hughes, C., Davidson, G., Pangelis, S. & Kennedy, S.J. (2015) A new neutron radiography/tomography/imaging station DINGO at OPAL. *Physics Procedia*, 69, 27–32.
Gardner, N.M., Holliday, C.M. & O'Keefe, F.R. (2010) The braincase of *Youngina capensis* (Reptilia, Diapsida): new insights from high-resolution CT scanning of the holotype. *Palaeontologia Electronica*, 13, 19A.
Georgi, J.A., Sipla, J.S. & Forster, C.A. (2013) Turning semicircular canal function on its head: dinosaurs and a novel vestibular analysis. *PLoS One*, 8, e58517.
Goyens, J. (2019) High ellipticity reduces semi-circular canal sensitivity in squamates compared to mammals. *Scientific Reports*, 9, 16428.
Grohé, C., Tseng, Z.J., Lebrun, R., Boistel, R. & Flynn, J.J. (2016) Bony labyrinth shape variation in extant Carnivora: a case study of Musteloidea. *Journal of Anatomy*, 228, 366–383.
Heaton, M.J. (1979) Cranial anatomy of primitive captorhinid reptiles from the Late Pennsylvanian and early Permian of Oklahoma and Texas. *Bulletin of the Oklahoma Geological Survey*, 127, 1–84.
Holly, C. (2004) Grouped ZProjector (for ImageJ), https://imagej.nih.gov/ij/plugins/group.html. Holly Mountain Software, Waterville, Maine, USA. Accessed Jan 21, 2017.
Hopson, J.A. (1979) Paleoneurology. *Biology of the Reptilia*, 9, 39–148.
Ivahknenko, M.F., Golubev, V.K., Gubin, Y.M., Kalandadze, N.N., Novikov, I.V., Sennikov, A.G. et al. (1997) Permian and Triassic tetrapods of eastern Europe. *Proceedings of the Palaeontological Institute of the Russian Academy of Sciences (GEOS) Moscow*, 268, 1–216. [in Russian]
Ivakhnenko, M.F. (2008) Cranial morphology and evolution of Permian Dinomorpha (Eotherapsida) of eastern Europe. *Paleontological Journal*, 42, 859–995.
Kemp, T.S. (2005) *The origin and evolution of mammals*. Oxford: Oxford University Press.
Kemp, T.S. (2016) Non-mammalian synapsids: the beginning of the mammal line. In: Clack, J.A., Fay, R.R. & Popper, A.N. (Eds.) *Evolution of the Vertebrate Ear – Evidence from the Fossil Record*. Springer International: Cham, Switzerland, pp. 107–137.
Klembara, J., Hain, M., Ruta, M., Berman, D.S., Pierce, S.E. & Henrici, A.M. (2020) Inner ear morphology of diadectomorphs and seymouriamorphs (Tetrapoda) uncovered by high-resolution X-ray micro-computed tomography, and the origin of the amniote crown group. *Palaeontology*, 63, 131–154.
Laaß, M. (2015a) Virtual reconstruction and description of the cranial endocast of *Pristerodon mackayi* (Therapsida, Anomodontia). *Journal of Morphology*, 276, 1089–1099.
Laaß, M. (2015b) Bone-conduction hearing and seismic sensitivity of the late Permian anomodont *Kawingasaurus fossilis*. *Journal of Morphology*, 276, 121–143.
Laaß, M. (2016) The origins of the cochlea and impedance matching hearing in synapsids. *Acta Palaeontologica Polonica*, 61, 267–280.
Langston, W. & Reisz, R.R. (1981) *Aerosaurus wellesi*, new species, a varanopseid mammal-like reptile (Synapsida: Pelycosauria) from the Lower Permian of New Mexico. *Journal of Vertebrate Paleontology*, 1, 73–96.
Lebrun, R., De León, M.P., Tafforeau, P. & Zollikofer, C. (2010) Deep evolutionary roots of strepsirrhine primate labyrinthine morphology. *Journal of Anatomy*, 216, 368–380.
Lieberman, D.E., Ross, C.F. & Ravosa, M.J. (2000) The primate cranial base: ontogeny, function, and integration. *Yearbook of Physical Anthropology*, 43, 117–169.
Liu, J., Rubidge, R. & Li, J. (2009) New basal synapsid supports Laurasian origin for therapsids. *Acta Palaeontologica Polonica*, 54, 393–400.
Luo, Z.-X. (2001) Inner ear and its bony housing in tritylodonts and implications for evolution of mammaliaform ear. *Bulletin of the Museum of Comparative Zoology*, 156, 81–97.

Luo, Z.-X. (2011) Developmental patterns in Mesozoic evolution of mammal ears. *Annual Review of Ecology, Evolution and Systematics*, 42, 355–380.

Luo, Z.-X., Schultz, J.A. & Ekdale, E.G. (2016) Evolution of the middle and inner ears of mammaliaforms: the approach to mammals. In: Clack, J.A., Fay, R.R. & Popper, A.N. (Eds.) *Evolution of the vertebrate ear – evidence from the fossil record*. Springer International: Cham, Switzerland, pp. 139–174.

Maddin, H.C., Jenkins, F.A. Jr & Anderson, J.S. (2012) The braincase of *Eocaecilia micropodia* (Lissamphibia, Gymnophiona) and the origin of caecilians. *PLoS One*, 7, e50743.

Maddin, H.C. & Sherratt, E. (2014) Influence of fossoriality on inner ear morphology: insights from caecilian amphibians. *Journal of Anatomy*, 225, 83–93.

Maho, S., Gee, B.M. & Reisz, R.R. (2019) A new varanopid synapsid from the early Permian of Oklahoma and the evolutionary stasis in this clade. *Royal Society Open Science*, 6, 191297.

Manley, G.A. (2012) Evolutionary paths to mammalian cochleae. *Journal of the Association for Research in Otolaryngology*, 13, 733–743.

Manoussaki, D., Chadwick, R.S., Ketten, D.R., Arruda, J., Dimitriadis, D. & O'Malley, J.T. (2008) The influence of cochlear shape on low-frequency hearing. *Proceedings of the National Academy of Sciences*, 105, 6162–6166.

Marino, L., Uhen, M.D., Pyenson, N.D. & Frohlich, B. (2003) Reconstructing cetacean brain evolution using computed tomography. *The Anatomical Record*, 272B, 107–117.

Mays, C., Bevitt, J.J. & Stilwell, J. (2017) Pushing the limits of neutron tomography in palaeontology: three-dimensional modelling of in situ resin within fossil plants. *Palaeontologia Electronica*, 20, article no. 3.57A.

Modesto, S.P., Sidor, C.A., Rubidge, B.S. & Welman, J. (2001) A second varanopseid skull from the Upper Permian of South Africa: implications for Late Permian 'pelycosaur' evolution. *Lethaia*, 34, 249–259.

Neenan, J.M. & Scheyer, T.M. (2012) The braincase and inner ear of *Placodus gigas* (Sauropterygia, Placodontia) – a new reconstruction based on micro-computed tomographic data. *Journal of Vertebrate Paleontology*, 32, 1350–1357.

Palci, A., Hutchinson, M.N., Caldwell, M.W. & Yee, M.S.Y. (2017) The morphology of the inner ear of squamate reptiles and its bearing on the origin of snakes. *Royal Society Open Science*, 4, 170685.

Pardo, J.D., Szostakiwskyj, M., Ahlberg, P.E. & Anderson, J.S. (2017) Hidden morphological diversity among early tetrapods. *Nature*, 546, 642–645.

Pusch, L.C., Ponstein, J., Kammerer, C.F. & Fröbisch, J. (2020) Novel endocranial data on the early therocephalian *Lycosuchus vanderrieti* underpin high character variability in early theriodont evolution. *Frontiers in Ecology and Evolution*, 7, 464.

Ramírez-Chaves, H.-E., Weisbecker, V., Wroe, S. & Phillips, M.J. (2016) Resolving the evolution of the mammalian middle ear using Bayesian inference. *Frontiers in Zoology*, 13, article 39.

Reisz, R.R. (1986). *Pelycosauria*, Vol. 17A. Handbuch der Paläoherpetologie. Stuttgart: Gustav Fischer Verlag, p. 102.

Reisz, R.R. & Berman, D.S. (2001) The skull of *Mesenosaurus romeri*, a small varanopseid (Synapsida: Eupelycosauria) from the Upper Permian of the Mezen River Basin, northern Russia. *Annals of Carnegie Museum*, 70, 113–132.

Reisz, R.R. & Dilkes, D.W. (2003) *Archaeovenator hamiltonensis*, a new varanopid (Synapsida: Eupelycosauria) from the Upper Carboniferous of Kansas. *Canadian Journal of Earth Science*, 40, 667–678.

Reisz, R.R., Dilkes, D.W. & Berman, D.S. (1998) Anatomy and relationships of *Elliotsmithia longiceps* Broom, a small synapsid (Eupelycosauria: Varanopseidae) from the late Permian of South Africa. *Journal of Vertebrate Paleontology*, 18, 602–611.

Reisz, R.R. & Modesto, S.P. (2007) *Heleosaurus scholtzi* from the Permian of South Africa: varanopid synapsid, not a diapsid reptile. *Journal of Vertebrate Paleontology*, 27, 734–739.

Rogers, S.W. (1999) *Allosaurus*, crocodiles, and birds: evolutionary clues from spiral computed tomography of an endocast. *The Anatomical Record*, 257, 162–173.

Romer, A.S. & Price, L.I. (1940) Review of the Pelycosauria. *Geological Society of America Special Papers*, 28, 1–534.

Rubidge, B.S. (1990) A new vertebrate biozone at the base of the Beaufort Group, Karoo Sequence (South Africa). *Palaeontologica Africana*, 27, 17–20.

Rubidge, B.S. (1995) Biostratigraphy of the Beaufort Group (Karoo Supergroup). *Geological Survey of South Africa, Biostratigraphic Series*, 1, 1–45.

Rubidge, B.S. & Sidor, C.A. (2001) Evolutionary patterns among Permo-Triassic therapsids. *Annual Review of Ecology and Systematics*, 32, 449–480.

Schade, M., Rauhut, O.W.M. & Evers, S.W. (2020) Neuroanatomy of the spinosaurid *Irritator challengeri* (Dinosauria: Theropoda) indicates potential adaptations for piscivory. *Scientific Reports*, 10, 9259.

Sereno, P.C., Wilson, J.A., Witmer, L.M., Whitlock, J.A., Maga, A., Ide, O. et al. (2007) Structural extremes in a Cretaceous dinosaur. *PLoS One*, 2, e1230.

Silcox, M.T., Bloch, J.I., Boyer, D.M., Godinot, M., Ryan, T.M., Spoor, F. et al. (2009) Semicircular canal system in early primates. *Journal of Human Evolution*, 56, 315–327.

Sobral, G. & Müller, J. (2019) The braincase of *Mesosuchus browni* (Reptilia, Archosauromorpha) with information on the inner ear and description of a pneumatic sinus. *PeerJ*, 7, e6798.

Sobral, G., Sookias, R.B., Bhullar, B.-A.-S., Smith, R., Butler, R.J. & Müller, J. (2016) New information on the braincase and inner ear of *Euparkeria capensis* Broom: implications for diapsid and archosaur evolution. *Royal Society Open Science*, 3, 160072.

Spindler, F., Werneburg, R., Schneider, J.W., Luthardt, L., Annacker, V. & Rößler, R. (2018) First arboreal 'pelycosaurs' (Synapsida: Varanopidae) from the early Permian Chemnitz Fossil Lagerstätte, SE Germany, with a review of varanopid phylogeny. *PalZ*, 92, 315–364.

Spoor, F., Bajpal, S., Hussaim, S.T., Kumar, K. & Thewissen, J.G.M. (2002) Vestibular evidence for the evolution of aquatic behaviour in early cetaceans. *Nature*, 417, 163–166.

Spoor, F., Garland, T., Krovitz, G., Ryan, M., Silcox, M.T. & Walker, A. (2007) The primate semicircular canal system and locomotion. *Proceedings of the National Academy of Science*, 104, 10808–10812.

Stokstad, E. (2003) Peering into ancient ears. *Science*, 302, 770–771.

Szostakiwskyj, M., Pardo, J.D. & Anderson, J.S. (2015) Micro-CT study of Rhynchonkos stovalli (Lepospondyli, Recumbirostra), with description of two new genera. *PLoS One*, 10, e0127307.

Vasilopoulou-Kampitsi, M., Goyens, J., Van Damme, R. & Aerts, P. (2019) The ecological signal on the shape of the lacertid vestibular system: simple versus complex microhabitats. *Biological Journal of the Linnean Society*, 127, 260–277.

Vaughn, P.P. (1958) A pelycosaur with supsphenoidal teeth from the lower Permian of Oklahoma. *Journal of the Washington Academy of Sciences*, 48, 44–47.

Walsh, S.A., Barrett, P.M., Milner, A.C., Manley, G. & Witmer, L.M. (2009) Inner ear anatomy is a proxy for deducing auditory capability and behaviour in reptiles and birds. *Proceedings of the Royal Society B*, 276, 1355–1360.

Walsh, S.A., Iwaniuk, A.N., Knoll, M.A., Bourdon, E., Barrett, P.M., Milner, A.C. et al. (2013) Avian cerebellar floccular fossa size is not a proxy for flying ability in birds. *PLoS One*, 8, e67176.

Witmer, L.M., Chatterjee, S., Franzosa, J. & Rowe, T. (2003) Neuroanatomy of flying reptiles and implications for flight, posture and behaviour. *Nature*, 425, 950–953.

Witmer, L.M., Ridgely, R.C., Dufeau, D.L. & Semones, M.C. (2008) Using CT to peer into the past: 3D visualization of the brain and ear regions of birds, crocodiles, and Nonavian dinosaurs. In: Endo, H. & Frey, R. (Eds.) *Anatomical imaging: towards a new morphology*. Tokyo, Japan: Springer-Verlag, pp. 67–87.

Yi, H. & Norell, M. (2019) The bony labyrinth of *Platecarpus* (Squamata: Mosasauria) and aquatic adaptations in squamate reptiles. *Palaeoworld*, 28, 550–561.

How to cite this article: Bazzana, K.D., Evans, D.C., Bevitt, J.J. & Reisz, R.R. (2022) Neurosensory anatomy of Varanopidae and its implications for early synapsid evolution. *Journal of Anatomy*, 240, 833–849. Available from: https://doi.org/10.1111/joa.13593